RESEARCH ARTICLE
doi: 10.2306/scienceasia1513-1874.2020.S005

ScienceAsia 46S (2020): **36–42**

Fluorescence determination of soluble pyrophosphate levels in synovial fluid as a marker of pseudogout using middle point of quantification concept and molecular sensor

Nattha Yongwattana[a], Nutsara Mekjinda[a], Wannee Thepsing[a], Supasara Ounsuk[a], Pravit Wongkongkatep[a], Tulyapruek Tawonsawatruk[b], Itaru Hamachi[c], Akio Ojida[d], Jirarut Wongkongkatep[a,*]

[a] Department of Biotechnology, Faculty of Science, Mahidol University, Bangkok 10400 Thailand
[b] Department of Orthopedics, Faculty of Medicine, Ramathibodi Hospital, Mahidol University, Bangkok 10400 Thailand
[c] Department of Synthetic Chemistry and Biological Chemistry, Graduate School of Engineering, Kyoto University, Kyoto 615-8510 Japan
[d] Graduate School of Pharmaceutical Sciences, Kyushu University, Fukuoka 812-8582 Japan

*Corresponding author, e-mail: jirarut.chu@mahidol.ac.th

Received 2 Nov 2019
Accepted 25 Feb 2020

ABSTRACT: Pseudogout is a type of joint inflammations caused by deposition of calcium pyrophosphate (CaPPi) crystals in the affected joint. As Ca^{2+} is abundant in the synovial fluid (SF), high levels of soluble PPi in the SF could be one of the key factors that contribute to CaPPi formation in the joint and may serve as a biomarker for pseudogout. Here, we developed and applied an artificial molecular sensor to selective fluorescent detection of soluble PPi in SF of the arthritis patients. The sensor employed xanthene as a fluorophore and the Dpa/Zn(II) as two specific binding sites for PPi. When titrated with serially diluted aqueous PPi solutions, the sensor displayed high sensitivity and exhibited the detection limit of 0.01 μM. The effect of salt concentration was normalized via the concept of Middle Point of Quantification (MPOQ) firstly proposed in this study. The performance of this sensor was also further validated by testing with SF samples extracted from eight clinical patients. The results revealed that six patients had the PPi levels in the range of 60 and 200 μM, indicating moderate likelihood of having pseudogout. Hence, our new method for determining the soluble PPi levels in SF shows promise as a robust, sensitive, and accurate diagnostic tool for the pseudogout.

KEYWORDS: pseudogout, calcium pyrophosphate crystal, synovial fluid, fluorescent detection, molecular sensor

INTRODUCTION

Nowadays, aging populations are growing rapidly in all parts of the world, and as a result, the numbers of elderly individuals inflicted with chronic diseases are also increasing. This recent trend calls for more effective, minimally invasive strategies to detect and treat chronic diseases in a timely manner. A disease that will gain benefit immensely from having efficient diagnostic platforms is pseudogout, an arthritic disease caused by deposition of calcium pyrophosphate crystals in the joints of elderly patients, outwardly manifested as swelling, redness, and pain in the affected areas [1, 2]. Specifically, inorganic pyrophosphate (PPi), generated from extracellular adenosine triphosphate (ATP), forms crystals with calcium in the pericellular matrix of articular cartilage [3, 4]. Thus, the concentration of soluble PPi in patient synovial fluid (SF) can be exploited as a biomarker for pseudogout diagnosis [5]. However, complicating detection of pseudogout is the fact that it highly resembles gout in appearance and symptoms. Both gout and pseudogout involve formation of crystals in joints, though for gout the crystals are monosodium urate [6]. At present, there are few diagnostic methods available to differentiate between gout and pseudogout, such as detection of crystals by radiography or polarized light microscopy, but unfortunately they can lead to misinterpretation due to the aforementioned similarities [1, 7]. Several PPi detection platforms have been developed [8–11] and some of them were applicable to the biological fluid such as serum [9], urine [12] and synovial

fluid [13]. However, there is no systematic investigation of using the molecular sensor as a PPi detection motif in SF, which is a marker of pseudogout. Therefore, this research aimed to apply xantheneDpa-Zn(II) complex [11] as a PPi-specific fluorescent sensor for the systematic determination of soluble PPi in SF of the arthritis patients. The effect of high salt content in SF has been normalized via the concept of MPOQ, enabling the reliable, rapid and specific method for soluble PPi detection. As a result, the xantheneDpa-Zn (II) complex holds potential for detection of pseudogout, without cross reactivity to gout and other joint inflammations.

MATERIALS AND METHODS

Chemicals and reagents

XantheneDpa-Zn(II) complex ($C_{39}H_{34}N_6O_4Zn_2 \cdot 2ClO_4 \cdot 3H_2O$), referred hereafter as Dpa sensor, was synthesized following Ojida et al [11]. Enliten kit was purchased from Promega, USA. HEPES ($C_8H_{18}N_2O_4S$), sodium pyrophosphate (NaPPi), adenosine triphosphate (ATP), adenosine diphosphate (ADP) and adenosine monophosphate (AMP) were available from Sigma-Aldrich. Hyaluronic acid sodium salt was purchased from Wako Chemicals, Japan. Other inorganic salts such as $MgCl_2$, $CaCl_2$, KCl and NaCl were available from Merck, Germany. All chemicals are of analytical grade with the purity of 99.5% or higher.

Formation of calcium pyrophosphate crystal in test tube

To the 40 mM HEPES buffer (pH 7.4) solution containing 136 mM NaCl, 4.0 mM KCl, 1.5 mM $CaCl_2$ and 1.03 mg/mL hyaluronic acid, NaPPi solution was added to the final concentration of 0–0.5 mM and then the solutions were kept in the incubator (JSR, JSSI-100c) under 37 °C. The white crystals were then filtered using Whatman No. 2 filter paper and dried under vacuum for 2 days. The FTIR analysis was performed by mixing the dried sample with KBr and analyzed by Perkin Elmer Frontier FTIR spectrometer. An epifluorescence microscope (Olympus BX 51 equipped with digital camera) was used to image the micro-scaled appearance of the crystals.

SF samples of patients with joint inflammation symptom

Patient SF was kindly provided by Asst. Prof. Dr. Tulyapruek Tawonsawatruk, Department of Orthopedics, Faculty of Medicine, Ramathibodi Hospital, Mahidol University, Bangkok, Thailand. These SF samples were the wastes from the therapeutic treatment of the patients with joint inflammation symptom, and showed no sign of bacterial infection. The obtained SF samples were used in accordance with the ethical approval of the Ramathibodi Hospital, Mahidol University, Bangkok, Thailand (Documentary Proof of Ethical Clearance Committee on Human Rights Related to Research Involving Human Subjects, based on the declaration of Helsinki, Faculty of Medicine Ramathibodi Hospital, Mahidol University Reference No. MURA2017/317). The SF samples were kept at −20 °C until analysis.

Analysis of soluble PPi concentration in the biological sample

The patient SF was pretreated by centrifugation at 12 000 rpm (9660×g) for 10 min, and the clarified supernatant was used for subsequent analysis of soluble PPi level. Briefly, the supernatant was serially diluted and an appropriate volume of each dilution was added to a solution of 1 μM Dpa sensor in 50 mM HEPES buffer (3 mL), pH 7.4, contained in a quartz cell at 25 °C. The serial diluents were added to the sensing solution in the order from low to high concentrations. The volume of the titrant was kept below 30 μL in order to constrain the volume change during the titration to 1%. Fluorescence spectra were then recorded on a spectrofluorometer (JASCO FP6500, Japan). The fluorescence spectra of the Dpa sensor before and after titration were referred as F_0 and F, respectively. The standard curve between fluorescent intensity and PPi concentrations was constructed from titration of the sensor with 0.01–5 μM standard solutions, using the same titration procedure as outlined.

To negate the effects of salts, MPOQ was used to calculate the concentration of PPi. The sample to be quantified was first serially diluted and sensed with Dpa sensor. The sigmoidal plot between F/F_0 and folds of dilution was generated. Then, three linear regression trendlines were drawn – one through the three lowest data points (bottom line), one through the inflection point (middle line), and one through the three highest data points (top line). The intersection between bottom and middle lines was designated as the Lower Limit of Quantification (LLOQ), whereas the intersection between middle and top lines was called the Upper Limit of Quantification (ULOQ). The point located halfway between LLOQ and ULOQ was the MPOQ. As the concentration of PPi at MPOQ was 0.9 μM in the case of Dpa sensor

and PPi titration under the similar salts contents to SF, the fold of dilution at MPOQ was used to back-calculate the soluble PPi concentration in the undiluted sample using the following equation.

$$[\mathrm{PPi}]_{\mathrm{MPOQ,SF}} = \frac{[\mathrm{PPi}]_{\mathrm{MPOQ,std}}}{\text{Dilution factor}}$$

Method validation using sodium pyrophosphate decahydrate ($Na_4O_7P_2 \cdot 10\,H_2O$, Sigma-Aldrich) as a standard demonstrated a high accuracy with an error of less than 7%.

Analysis of ATP concentration in patient SF

The standard curve of ATP was constructed using Enliten kit. ATP standard (10^{-7} M), provided in the Enliten kit, was diluted to 10^{-17} M in ATP-free water. Luciferase/Luciferin solution (50 µL) and the serially diluted ATP standards (10^{-7}–10^{-17} M) (5 µL) were pipetted into 384-well plate and analyzed for the luminescence intensity using a microplate reader (TECAN Spark 10M, Tecan Group Ltd., Mannedorf, Switzerland). The amounts of ATP in patient SF were determined at 0, 1, 2, 3, 4, 5, 6, 24 h after transferring from −20 °C to room temperature at 25 °C, by comparing luminescent readouts to the standard curve.

RESULTS AND DISCUSSION

Sensitivity and selectivity of the sensor

Analysis of the PPi content in biological fluids such as SF is difficult compared to simple buffer systems because biological milieu often contains various concentrations of ions, proteins and glucose. According to McMahon et al [14], the inorganic composition of SF is as follows: sodium-136.1, calcium-1.2–2.4, bicarbonate-9.7–15.4 and chloride-107.1 mM with a small amount of potassium. Total protein content of 1.72 g/L was reported, in which 55–70% represented albumin, while 0.3–0.4 g/L of hyaluronic acid and 70–110 mg/L of glucose were also detected in the SF. Therefore, a highly sensitive and specific molecular sensor is critical in ensuring that interferences due to these background molecules are minimal or absent. Among sensors in our previously synthesized library, the xanthene-based Dpa sensors employed in this study exhibited the highest sensitivity and selectivity in PPi detection, which could be explained by its unique sensing mechanism, i.e., pyrophosphate binds to the two zinc ions and pull them away from the oxygen, triggering the reversible deoxygenation and hence formation of the highly fluorescent xanthene, as illustrated in Fig. 1a and previously described in details by Ojida et al [10] and Wongkongkatep et al [11]. Addition of 2 µM PPi increased the fluorescence emission at the maximum wavelength (521 nm) of the Dpa sensor (1 µM) by up to 126-fold (Fig. 1b, inset), while addition of ATP and ADP yielded only 16- and 13-fold increases, respectively. In addition, the sensor showed no fluorescence response with urate associated with gout, and other common ions including phosphate, acetate, nitrate, carbonate and sulfate (Fig. 1b).

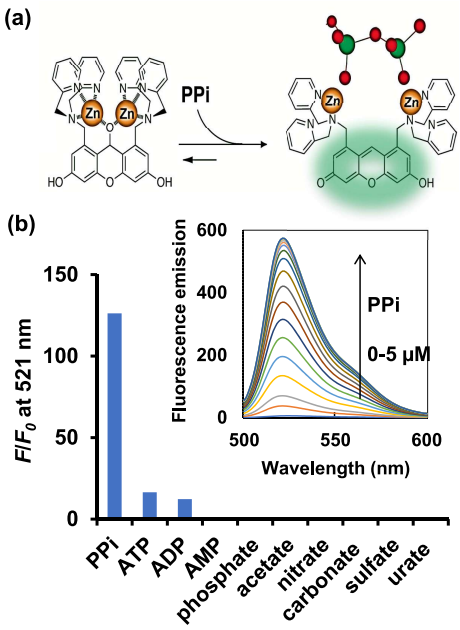

Fig. 1 (a) Sensing mechanism of Dpa sensor toward PPi and (b) selectivity of the Dpa sensor (1 µM) upon addition of various anions (2 µM) measured in 50 mM HEPES buffer, 10 mM NaCl, 1 mM $MgCl_2$ (pH 7.4, 25 °C), λ_{ex} 488 nm. Inset: Fluorescence emission of Dpa sensor (1 µM) upon addition of PPi in 50 mM HEPES buffer, 10 mM NaCl, 1 mM $MgCl_2$ (pH 7.4, 25 °C).

Table 1 The threshold concentration of soluble PPi level estimated in artificial SF.

PPi level	Risk of pseudogout
< 60 µM	No risk [16]
60–200 µM	Moderate risk: crystals may form over a long term
> 200 µM	High risk: crystals may form within 3 days

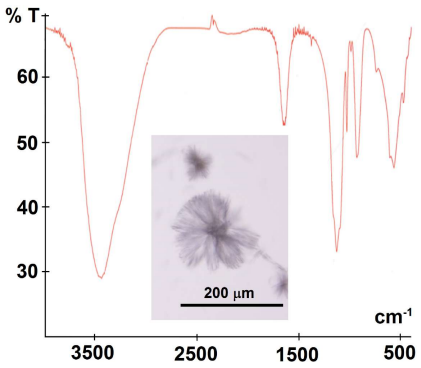

Fig. 2 FTIR spectra (KBr) and physical appearance (inset) of the CaPPi crystal prepared in artificial SF.

Formation of calcium pyrophosphate crystal in the artificial SF

Crystallization of CaPPi was performed in artificial SF in a test tube to simulate the pathogenesis of pseudogout. To artificial synovial solution containing salts and hyaluronic acid, soluble NaPPi solution was added to the final concentration of 0–500 μM and the solutions were kept static under 37 °C. White precipitate of calcium pyrophosphate was observed starting on day 3, in samples with 200 μM PPi or above. Epifluorescence microscope revealed flower-like crystals characteristic of CaPPi (Fig. 2). In addition, the FTIR spectra of dried CaPPi crystals exhibited peaks between 400–600 and 1000–1200 cm^{-1}, signature of PO_4^{-3} groups (Fig. 2) and in good agreement with the previous report by Rosenthal et al [15]. Taken together, our results confirmed that CaPPi could crystallize in artificial SF. It has been reported that CaPPi crystals were allowed to dissolve in 100 mM Tris-HCl buffer solution (pH 7.4) at 37 °C, and after 8 h of incubation, the dissolved CaPPi reached the equilibrium concentration of 60 μM [16]. This finding suggests that, for crystallization to occur, the concentration of PPi must exceed 60 μM. As an additional validation, we prepared CaPPi crystals by adding PPi to SF to the final concentration of 0.5 mM, and then allowing the solution to crystallize (sample A). The concentration of soluble PPi once the crystallization reaches equilibrium corresponds to its saturation concentration. We also prepared a negative control in which SF contained only 0.1 mM PPi and did not undergo crystallization (sample B). After crystals were removed, the clarified sample A was used to titrate a solution containing Dpa sensor, yielding the maximum F/F_0 of 96, whereas titration with sample B achieved the maximum F/F_0 of 82 (Fig. 3a). The higher maximum F/F_0 value of sample A indicates that the equilibrium concentration of PPi must be above 100 μM. In conjunction with our finding that the initial PPi concentration of at least 200 μM was required for crystallization in artificial SF; the saturation concentration of PPi in this matrix likely lies within the 100–200 μM range, which is slightly higher than the reported value of 60 μM PPi [16]. This discrepancy could be due to supersaturation, which is not uncommon in crystallization experiments. Nonetheless, CaPPi concentrations below 60 μM should be far enough from the saturation point and thus presumably pose no risk for pseudogout [16]. On the other hand, CaPPi concentrations above 200 μM will certainly exceed the saturation point and thus enable crystallization. We thereby propose classification of pseudogout risk into 3 levels based on concentrations of PPi in SF, as shown in Table 1.

Effects of salts in PPi level analysis

However, the sensitivity of Dpa sensor was influenced by salt content as the decrease in the maximum F/F_0 was observed, which can be attributed to the high levels of salts present in artificial SF. Because the salt content in the artificial SF prepared in this study was 136 mM Na^+, 4 mM K^+, 1.5 mM Ca^{2+} and 143 mM Cl^-, the effects of salts on the performance of the Dpa sensor should be evaluated thoroughly. In the absence of NaCl or $CaCl_2$, 2 μM of PPi enhanced the fluorescence emission of the Dpa sensor (1 μM) by 126 folds, whereas only 43-fold increase was achieved when 100 mM of NaCl was included (Fig. 3b). Divalent anions such as Ca^{2+} further exacerbated the signal inhibition. For instance, 100 mM $CaCl_2$ lowered the increase in F/F_0 of the Dpa sensor to merely 11 folds, while 500 mM $CaCl_2$ nearly abolished the increase (Fig. 3b). Considering the negative effects of salts on the Dpa sensor, a PPi sensing system that is impervious to the effects of salts would be highly desirable for applications in the biological fluids, where presence of salts are often unavoidable.

Analysis of soluble PPi concentration in patient SF

Although high salt concentrations reduced the signal amplitude, they did not influence the dynamic range of the Dpa sensor. Therefore, it should be possible to correct for the effect of salts in PPi detection, taking advantage of the fact that the concentration of PPi at the MPOQ was approximately

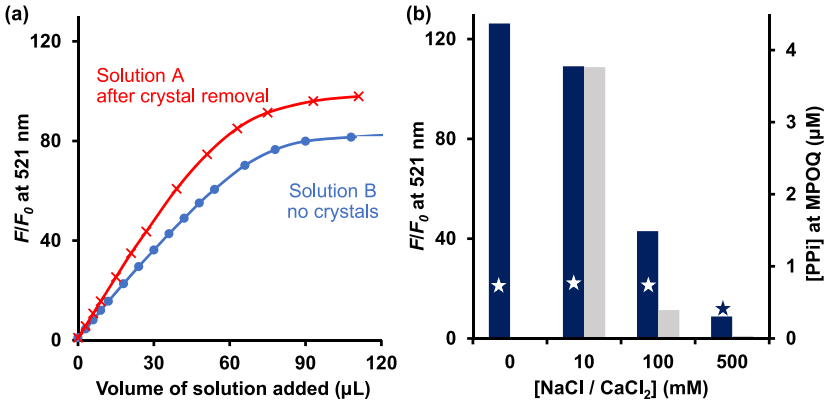

Fig. 3 (a) Fluorescence titration of the artificial SF after CaPPi crystal formation at the initial soluble PPi concentration of 0.5 mM (red cross) and 0.1 mM (blue circle) to the 50 mM HEPES buffer (pH 7.4), 10 mM NaCl, 1 mM $MgCl_2$ and (b) effects of various concentrations of NaCl (dark blue) and $CaCl_2$ (light grey) on the F/F_0 (bar graph) and MPOQ (star) of the solution containing Dpa sensor (1 μM) and soluble PPi (2 μM). Measurement condition: 25 °C, λ_{ex} = 488 nm.

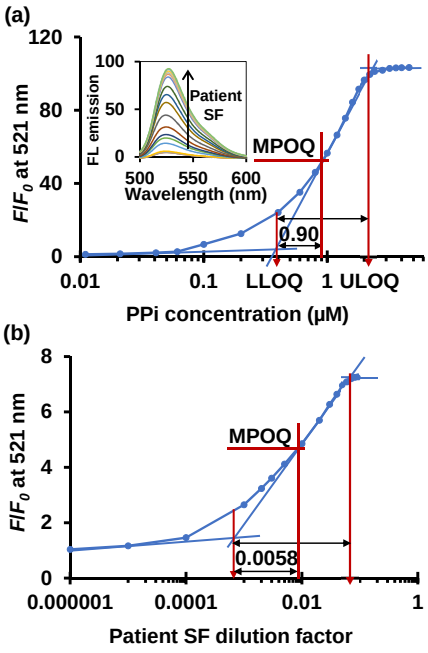

Fig. 4 (a) Standard curve of MPOQ calculation based on F/F_0 value of Dpa sensor (1 μM) in relationship with PPi added (0–5 μM) and fluorescence spectrum of the Dpa sensor (1 μM) when the patient SF was added (inset). (b) Change in fluorescence emission F/F_0 at 521 nm upon addition of serially diluted patient SF. Measurement conditions: 50 mM HEPES (pH 7.4), λ_{ex} = 488 nm, 25 °C.

0.90–0.93 μM regardless of the F/F_0 values at salt concentrations ranged from 0–100 mM (Fig. 3b). To determine the concentration of PPi at MPOQ, the reference curve was constructed by titrating Dpa sensor with a wide range of PPi concentrations. Following the steps for MPOQ analysis outlined in Materials and Methods, the LLOQ, MPOQ, and ULOQ were found to be 0.4, 0.9, and 2.2 μM respectively (Fig. 4a).

Table 2 The concentrations of soluble PPi determined in 8 patient SF samples using the Dpa sensor. Data was average ± SD of three individual replicates.

Sample No.	Maximum F/F_0	MPOQ	Concentration of PPi (μM)
1	7.24 ± 0.51	0.0058 ± 0.0002	155 ± 3.6
2	9.97 ± 0.59	0.0090 ± 0.0004	100 ± 6.7
3	21.34 ± 0.80	0.0092 ± 0.0003	97 ± 3.8
4	19.66 ± 0.90	0.0230 ± 0.0004	39 ± 2.2
5	4.86 ± 1.06	0.0050 ± 0.0003	180 ± 21.2
6	8.03 ± 0.42	0.0090 ± 0.0002	100 ± 2.9
7	718.84 ± 0.32	0.0180 ± 0.0002	50 ± 0.1
8	12.63 ± 0.63	0.0088 ± 0.0005	102 ± 10.5

With the PPi concentration at MPOQ elucidated, we proceeded to analyze 8 patient SF samples with the MPOQ analysis. Due to rarity of pseudogout cases in Thailand, we were unable to procure clinical samples from pseudogout patients, and samples from arthritic patients were used as substitutes. Each sample was serially diluted and added to the solution Dpa sensor in 50 mM HEPES buffer (pH 7.4). In all of the samples, the plot between F/F_0 and folds of dilution followed a sigmoidal pattern, indicating that soluble PPi was present in every sample (Fig. 4b). Notably, the maximum F/F_0 values varied largely between 4.86–21.34 (Table 2), possibly owing to the unequal interference from

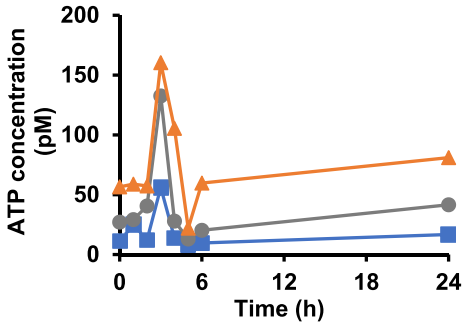

Fig. 5 ATP concentrations measured in the samples of patient SF No. 1 (orange triangle), No. 2 (blue square) and No. 4 (grey circle) over the course of 24 h after transferring from −20 °C storage to 25 °C.

salts across the samples. Using the MPOQ analysis, the soluble PPi concentrations in patient SF were found to range between 39 and 180 μM (Table 2). Two of the samples contained less than 60 μM PPi, indicating no risk of pseudogout based on the risk categories shown in Table 1. In the remaining 6 samples, the PPi content was between 60 and 200 μM, suggesting the moderate possibility of pseudogout. Therefore, this approach offers a sensitive and robust way to measure PPi and likelihood of pseudogout in biological samples, although it should be further validated using the reference material of PPi and the SF from actual pseudogout patients. It should be noted that it is essential to obtain the exact MPOQ of each sample by titration of the sample until its clear saturation point.

Analysis of ATP concentration in patient SF

Because ATP can induce moderate fluorescence signal from the Dpa sensor, as clearly shown in Fig. 1b, we sought to verify whether the ATP levels in our patient SF samples were high enough to interfere with the analysis. Using an ATP specific Luciferin/Lucierase assay, we measured the time-course of ATP concentrations produced in the patient SF samples gradually thawing at 25 °C. The assay revealed that the initial concentrations of ATP in three patient SF samples were in picomolar levels. The highest ATP concentrations (approximately 56–160 pM) were attained at 3 h in the experiment, when the patient SF had completely thawed (Fig. 5), but the ATP levels declined after this point, possibly due to certain ATP-consuming enzymes that survived during the storage at −20 °C. Notably, the highest concentrations of ATP acquired in this experiment were approximately three orders of magnitude below the lower detection limit of the Dpa sensor. Thus, the negligible presence of ATP in SF should not interfere with PPi detection by this sensor.

CONCLUSION

In summary, we have demonstrated that the Dpa sensor can be applied in quantification of soluble PPi content in SF. The method has the lower detection limit of 0.01 μM PPi and shows no or negligible responses to anionic species commonly present in biological matrices. The negative effects of high salts to the sensor's fluorescent responses were also successfully normalized using the concept of MPOQ. The concentration range of PPi that enables crystallization in artificial SF was estimated, although the survey of PPi concentrations in actual pseudogout patients is still required in order to establish the threshold value that distinguishes the pseudogout and normal cases. Taken together, fluorescent detection of soluble PPi using the Dpa sensor is a rapid, specific and sensitive method that holds promise for precise and accurate diagnosis of pseudogout.

Acknowledgements: This research was supported by Center of Excellence on Medical Biotechnology (CEMB), S&T Postgraduate Education and Research Development Office (PERDO), Office of Higher Education Commission (OHEC), Thailand. NM is grateful to RGJ Ph.D. Programme (PHD/1086/2557). This research is partially supported by the Faculty of Science, Mahidol University and the Thailand Research Fund (IRG5980001).

REFERENCES

1. Rosenthal AK, Ryan LM (2016) Calcium pyrophosphate deposition disease. *N Engl J Med* **374**, 2575–2584.
2. Hearn PR, Russell RG (1980) Formation of calcium pyrophosphate crystals in vitro: implications for calcium pyrophosphate crystal deposition disease (pseudogout). *Ann Rheum Dis* **39**, 222–227.
3. Costello JC, Rosenthal AK, Kurup IV, Masuda I, Medhora M, Ryan LM (2011) Parallel regulation of extracellular ATP and inorganic pyrophosphatase: Roles of growth factors, transduction modulators, and ANK. *Connect Tissue Res* **52**, 139–146.
4. Rosenthal AK, Gohr CM, Mitton-Fitzgerald E, Lutz MK, Dubyak GR, Ryan LM (2013) The progressive ankylosis gene product ANK regulates extracellular ATP levels in primary articular chondrocyte. *Arthritis Res Ther* **15**, ID R154.
5. Doherty M, Chuck A, Hosking D, Hamilton E (1991) Inorganic pyrophosphate in metabolic diseases predisposing to calcium pyrophosphate dihydrate crystal deposition. *Arthritis Rheum* **34**, 1297–1303.

6. Stanway J, Marianayagam T, Ellis S (2018) Crystal arthropathies. *Medicine* **46**, 181–186.
7. Zell M, Zhang D, FitzGerald J (2019) Diagnostic advances in synovial fluid analysis and radiographic identification for crystalline arthritis. *Curr Opin Rheumatol* **31**, 134–143.
8. Chatphueak N, Suksai C (2019) Water soluble dinuclear zinc(II) complex based sensor for pyrophosphate anion under indicator displacement assays. *Polyhedron* **170**, 742–748.
9. Xu X, Ren D, Chai Y, Cheng X, Mei J, Bao J, Wei F, Xu G, et al (2019) Dual-emission carbon dots-based fluorescent probe for ratiometric sensing of Fe(III) and pyrophosphate in biological samples. *Sensor Actuat B Chem* **298**, ID 126829.
10. Wongkongkatep J, Ojida A, Hamachi I (2017) Fluorescence sensing of inorganic phosphate and pyrophosphate using small molecular sensors and their applications. *Top Curr Chem* **375**, ID 30.
11. Ojida A, Takashima I, Kohira T, Nonaka H, Hamachi I (2008) Turn-on fluorescence sensing of nucleoside polyphosphates using a xanthene-based Zn(II) complex chemosensor. *J Am Chem Soc* **130**, 12095–12101.
12. Kong C, Liu Q, Li W, Chen Z (2019) Single particle-based colorimetric assay of pyrophosphate ions and pyrophosphatase with dark-field microscope. *Sensor Actuat B Chem* **299**, ID 126999.
13. Kiran S, Khatik R, Schirhag R (2019) Smart probe for simultaneous detection of copper ion, pyrophosphate, and alkaline phosphatase in vitro and in clinical samples. *Anal Bioanal Chem* **411**, 6475–6485.
14. Yavorskyy A, Hernandez-Santana A, McCarthy G, McMahon G (2008) Detection of calcium phosphate crystals in the joint fluid of patients with osteoarthritis-analytical approaches and challenges. *Analyst* **133**, 302–318.
15. Rosenthal AK, Mattson E, Gohr CM, Hirschmugl CJ (2008) Characterization of articular calcium-containing crystals by synchrotron FTIR. *Osteoarthr Cartil* **16**, 1395–1402.
16. Bennett RM, Lehr JR, McCarty DJ (1975) Factors affecting the solubility of calcium pyrophosphate dihydrate crystals. *J Clin Invest* **56**, 1571–1579.